

Dielectric-permittivity-driven charge carrier modulation at oxide interfaces

Wolter Siemons,^{1,2} Mark Huijben,¹ Guus Rijnders,¹ Dave H. A. Blank,¹ Theodore H. Geballe,² Malcolm R. Beasley,² and Gertjan Koster^{1,2,*}

¹*Faculty of Science and Technology and MESA+ Institute for Nanotechnology, University of Twente, 7500 AE Enschede, The Netherlands*

²*Geballe Laboratory for Advanced Materials, Stanford University, Stanford, California 94305, USA*

(Received 1 June 2010; published 22 June 2010)

High-quality bilayers of La-doped SrTiO₃ (STO) and LaAlO₃ (LAO) on SrTiO₃ have been grown controlling the location and behavior of the charge carriers by changing the thicknesses of the layers, which are dielectrically mismatched. In this system, the charge carriers are created at the La:STO/LAO interface and spread out toward the substrate due to the increase in dielectric constant as the temperature is lowered. When the electrons reach the interface of the La:STO and the pure STO, they display enhanced mobility in the quantum well at that interface for specific thicknesses.

DOI: [10.1103/PhysRevB.81.241308](https://doi.org/10.1103/PhysRevB.81.241308)

PACS number(s): 73.40.-c, 73.50.-h

Two dimensional electron gases (2DEGs) have been intensely investigated in conventional semiconductors in the last decades¹ but recently a 2DEG was also reported at the interface between two oxide semiconductors ZnO and Mg_xZn_{1-x}O.² Subsequently more systems showing two-dimensional behavior have been investigated, most notably the observed delta doping in a Nb-doped SrTiO₃ (STO) layer.³ These 2DEGs open the door to modulation doping schemes in which charge carriers are moved away from the defects that created them to form an electron gas at a location with a lower defect density. A quantum well has been demonstrated in LaAlO₃/LaVO₃/LaAlO₃ (LAO) samples by Higuchi *et al.*⁴ In these systems charge is created in a well, or at an interface, and shows two-dimensional behavior. However, an alternative approach is to create charge at one interface and transfer it to another (cleaner) interface. In oxides the possibility exists to find a material with a large variation in dielectric properties as a function of the temperature, for example, the dielectric constant of SrTiO₃ is approximately 20 000 at 4 K,⁵ compared to 300 at room temperature, which enhances the electron screening and allows electrons to spread out over large distances. This offers possibilities to enhance charge carrier modulation beyond those in conventional semiconductors as we will demonstrate using the interface between STO and LAO.

The observed conductivity when two nominal insulators, STO and LAO, form an interface^{6,7} has resulted in many experimental and theoretical studies (see Huijben *et al.*⁸ for one recent overview). In this Rapid Communication, we add an additional layer between the LAO and STO consisting of La-doped SrTiO₃ (La:STO) which displays enhanced scattering, suppressed electron mobilities, and carrier localization at low temperatures. This structure allows us to move the electrons away, due to the increased electronic screening as the dielectric constant in STO becomes larger at lower temperature, from the La:STO/LAO interface and form a highly mobile electron gas deeper in the sample at the other interface. We can control the location of the electrons by varying either the thickness of the low mobility La:STO layer or the top LAO layer. The La:STO thickness allows us to change the position of the STO/La:STO interface in the distribution and thereby probe the distribution at different locations whereas

the LAO thickness allows us to change the distribution of the electrons where thicker LAO layers move the electrons deeper into the structure. This model is schematically presented in Fig. 1 and will be described in quantitative detail later in this Rapid Communication.

The films used in our experiments were grown by pulsed laser deposition. The samples were grown in a vacuum chamber with a background pressure of 10⁻¹⁰ Torr. A 248 nm wavelength KrF excimer laser was employed with typical pulse lengths of 20–30 ns. The energy density on the target was kept at approximately 1.2 J/cm². All films were grown on TiO₂ terminated STO,⁹ at 815 °C in 10⁻⁵ Torr oxygen pressure with a laser repetition rate of 1 Hz. Reflection high-energy electron diffraction (RHEED) was used to keep track of film thickness and surface quality. La:STO was ablated from a sintered pressed target with 5% La doping. After deposition of the La:STO layer the sample was annealed in atomic oxygen. With the microwave generator set to 600 W and a flow of 2.5 ml/min this resulted in a flux of ~10¹⁷ oxygen atoms cm⁻² s⁻¹ (Ref. 10) while the background pressure remained at 10⁻⁵ Torr. After this oxidation step the samples were found to show insulating behavior caused by charge carrier freeze out by performing

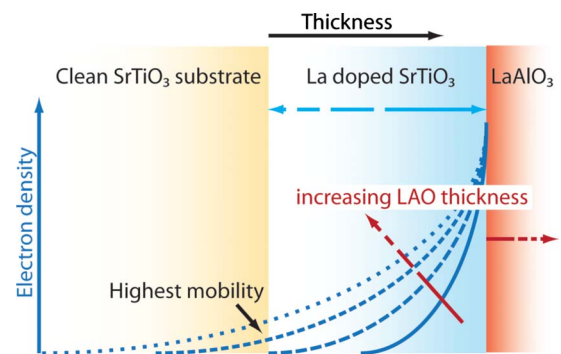


FIG. 1. (Color online) Schematic picture of the structure showing the dependence of the electron distribution on the LAO layer thickness. It also shows how the La:STO thickness moves the La:STO/STO interface through this distribution allowing us to probe the distribution by changing the La:STO thickness.

temperature-dependent transport measurements on samples at this stage. In the experiments to follow we will use this information to determine which part of the electrons are in the La:STO layer (these are localized at low temperatures) and which are in the STO substrate where carrier freeze out is usually not observed. The subsequent deposition of the LaAlO₃ layer was performed at 815 °C and 10⁻⁵ Torr oxygen pressure by ablating from a single-crystal target. The laser settings were the same as for the La:STO layer. After deposition the sample was cooled to room temperature under deposition pressure. The RHEED specular spot intensity oscillations and an atomic force micrograph are shown in the supplementary material¹¹ for a sample with 5 monolayers (ML) of La:STO and 5 ML of LAO. The transport measurements were performed in a Quantum Design physical property measurement system. Sheet resistance and carrier density were determined using the Van der Pauw technique.¹²

The two layer thicknesses have been changed systematically to study the transport properties of this system. For the first series of samples the La:STO layer thickness was kept constant at 10 ML and the LAO layer was varied from 4 to 6 ML. Their transport properties are shown in Figs. 2(a) and 2(b). The 4 ML LAO sample shows clear insulating behavior, which was very different from what is expected at LAO/STO interfaces (no La:STO) where the metal-insulator transition takes place between 3 and 4 ML.¹³ The insulating behavior is caused by localization (carrier freeze out) of the charge carriers as displayed in Fig. 2(b). The same happens for the sample with 5 ML of LAO. From an Arrhenius plot of the carrier density, see the inset of Fig. 2(b), we can determine the activation energy of the carriers to be 1.6 meV, a much lower energy than the 6 meV measured for undoped STO,^{14,15} which shows shallow donor sites are present. For a sample with 6 ML of LAO on top the behavior is fully metallic down to the lowest temperatures.

A second series consisted of samples with only 5 ML of La:STO. The transport properties of these samples are given in the supplementary information. As a function of LAO thickness we observe the same qualitative behavior as for the samples with 10 ML La:STO. However, we note the first film to display metallic behavior to the lowest temperatures is covered with 5 ML LAO, compared to 6 ML for the samples with 10 ML La:STO, and 4 ML for samples without any La:STO.

We know from the earlier discussed annealing experiments on La:STO that the electrons in the La:STO layer will be localized at low temperatures whereas the electrons which spread out beyond the La:STO will remain mobile to the lowest temperatures as is the case if there were no La:STO layer. Our model shows the thickness of the LAO layer will change the distribution of electrons. A thicker LAO layer allows the electrons to spread out further. This implies a thicker LAO layer is necessary to measure metallic behavior at the lowest temperatures when we make the La:STO layer thicker, which is exactly what we observed in the previous experiments.

We can make this more quantitative by calculating the spread of the electrons with the aid of a simple qualitative model based on a numerical solution of Poisson's equation following the approach used for a different materials

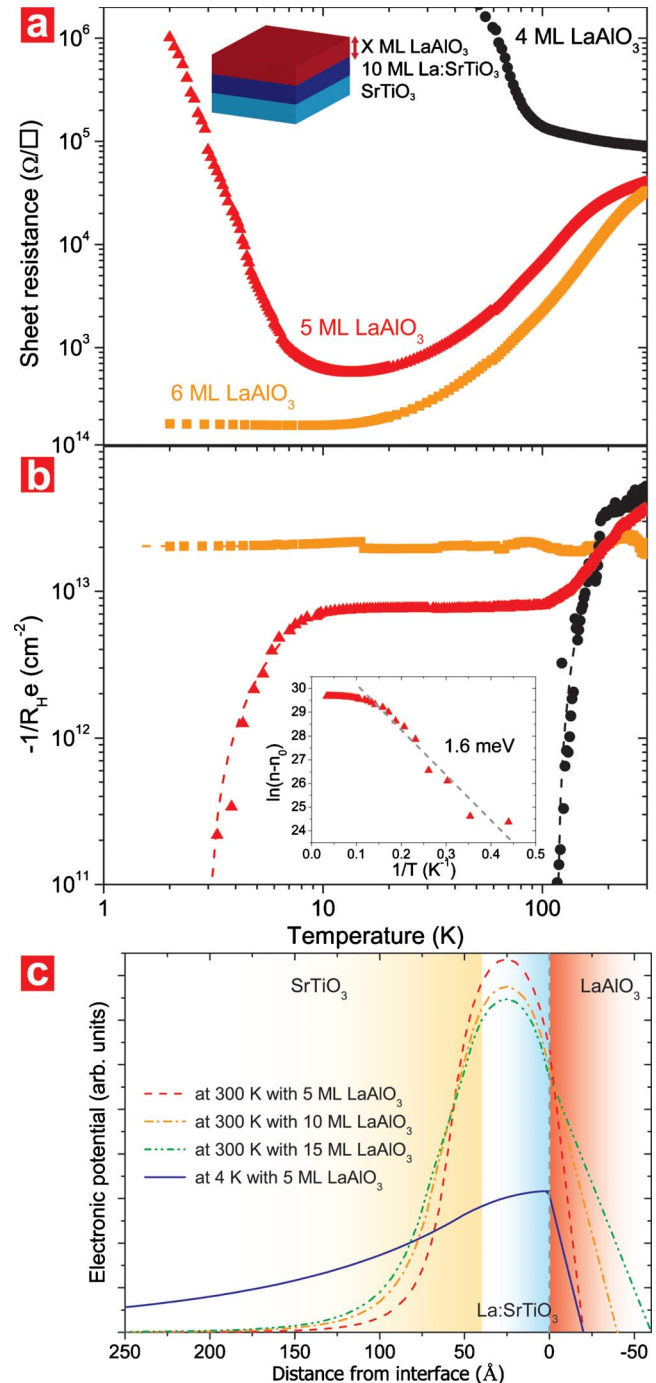


FIG. 2. (Color online) Transport properties taken during cooling: (a) sheet resistance and (b) sheet carrier density of films with 10 ML La:STO and 4, 5, and 6 ML of LaAlO₃ on top. The inset in (a) shows the schematic layout of the samples and the inset in (b) shows an Arrhenius plot of the 5 ML LAO sample. (c) The solution for the potential from Poisson's equation for samples with various LAO thicknesses and temperatures. For simplicity the La:STO and STO properties have been assumed to be the same. Assuming different properties will change the results quantitatively but qualitatively the trends remain the same. Thicker LAO layers allow the electrons to move further into the STO (here only shown at room temperature, at low temperature a similar effect is observed) but lowering the temperature (and increasing the dielectric constant) proves to be a much stronger effect.

system:¹⁶ the electric fields on both sides of the interface should satisfy $\epsilon_1 E_1 = \epsilon_2 E_2$ and the potential should be zero at the interfaces with vacuum. The electronic potentials calculated with this model are given in Fig. 2(c) for various LAO layer thicknesses. The electric field in the LAO will depend on the potential at the interface and the thickness of the LAO layer. A lower electric field in the LAO will cause the carriers to spread out more in this model, which is consistent with our observations. The main differences with the model used before¹⁶ are that here the LAO thickness is varied and shown to have a strong influence and that the additional layer of doped STO will have a shifted Fermi level which creates a second quantum well, which will be discussed in more detail later. This model does not rely on the existence of a build-in electric field. (Note that Segal *et al.*¹⁷ have shown there is no evidence from photoemission of a build-in field in the LAO.) The field in the LAO is due to the boundary condition which states the potential on the surface of the LAO and the potential deep inside the substrate need to be equal (in this case $V=0$).

Next we will focus on varying the La:STO thickness from 3 to 20 ML while keeping the LAO layer constant at 5 ML. We also include a 0 ML case, for which the La:STO growth and the annealing step are skipped but where the growth of the LAO layer was kept the same. In this experiment we keep the distribution of the electrons the same but change the fraction of electrons which is in the La:STO layer. The effect of the La:STO layer thickness on the transport properties is summarized in Fig. 3.

In the top panel of Fig. 3 the dependence of the residual sheet resistance ratio (RSRR) is shown. The RSRR goes down as the La:STO layer thickness increases. This reduction in RSRR is not caused by an increase in the sheet resistance at room temperature, which is 29–45 $\text{k}\Omega/\square$ for all samples. However, the low-temperature sheet resistance increases systematically causing the drop in RSRR. The 0 ML sample is clearly different, the low-temperature sheet resistance value extrapolates well but the room-temperature resistance is much lower.

In the lower panel are the dependencies of the sheet carrier density and the mobility of the charge carriers are given. The sheet carrier density is given per monolayer of La:STO to make it easy to compare with the theoretical sheet carrier density of 3×10^{13} per monolayer of 5% doped La:STO. To obtain the sheet carrier density for the total layer the value in the graph has to be multiplied with the number of MLs for that specific sample on the x axis. Mobility is high for the 0 ML case and decreases steadily as the layer becomes thicker. It rises again, however, after 5–10 ML where it peaks before it decreases again for the thicker samples. There is also a trend in the carrier densities at 300 and 20 K. For the 0 ML and thin La:STO samples few carriers are frozen out, i.e., the blue (circles) and red (squares) data points coincide. From 5 ML on a portion of the carriers is frozen out and for the 10 ML sample the freeze out reaches a maximum. Thicker samples show a lower percentage of carriers frozen out at 20 K but as said before these carriers display low mobilities at low temperature.

The increase in room-temperature resistance when the La:STO layer is introduced suggests all the carriers are in the

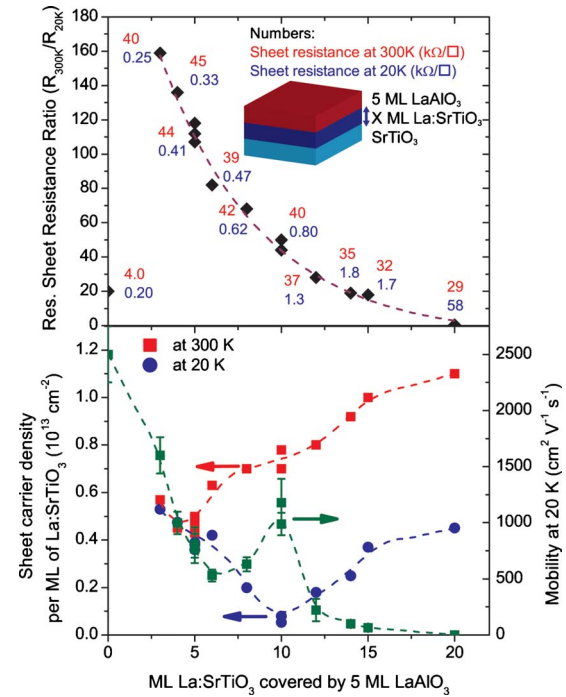


FIG. 3. (Color online) A summary of the transport properties of samples with a constant LAO thickness of 5 ML and a variable La:STO thickness. In the top panel the residual resistance ratio is given together with the values for the sheet resistance at 300 and 20 K. In the bottom panel the number of carriers at 300 and 20 K are plotted as well as the mobility of the electrons at 20 K.

La:STO layer at this temperature since La:STO is known to have a much higher resistivity than lightly doped STO.¹⁸ We note the sheet resistance at room temperature does not change significantly as the La:STO layer thickness is increased, consistent with all the carriers being in the La:STO for all layer thicknesses at room temperature. For the 0 ML sample there is no La:STO to increase scattering at room temperature, resulting in a lower sheet resistance for this sample. When the temperature is lowered and thus the dielectric constant increased (in undoped STO from some 300 at room temperature to over 10 000 at low temperatures and in La:STO from 200 at room temperature to 700 at low temperature¹⁹) the electrons are better screened and can spread out more in the material.¹⁶ For thin La:STO layers the electrons can easily reach the undoped STO substrate and attain high mobility due to the lack of scattering sites there. The low-temperature resistances extrapolate well to the 0 ML sample where all the carriers are in the undoped STO. When the La:STO layer is made thicker a larger fraction of the electrons will be in the La:STO layer resulting in a higher resistance due to increased impurity scattering in this layer. For large layer thicknesses all the electrons are localized in the La:STO layer (for the samples ranging from 12 to 15 ML this happens at a temperature lower than 20 K), and we also observe semiconducting behavior for the 20 ML sample. For intermediate thickness samples a break of the mobility trend is observed; From 5 to 10 ML of La:STO the electron mobility at low temperature actually increases. This behavior can be explained by looking at the electronic band diagram.

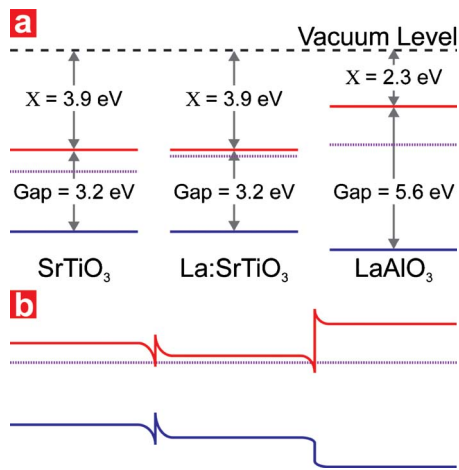


FIG. 4. (Color online) (a) The valence- and conduction-band arrangement for the three materials individually with the relevant parameters, where the dotted line is the Fermi level. (b) The reconstructed band picture after alignment of the Fermi level.

In Fig. 4(a) the electronic band parameters are given for the individual layers which results in the band diagram illustrated in Fig. 4(b) when they are brought into contact. The band diagram shows that in addition to the potential well at the La:STO/LAO interface there is a well at the STO/La:STO interface. For the sample with 10 ML of La:STO the majority of the electrons are frozen out in the La:STO and

the small portion that remains sits in this second well where it becomes a highly mobile electron gas.

To conclude, we have studied the properties of the interface between STO and LAO by inserting an extra layer of La-doped STO between the two. We observe the electrons are spreading out more when the LAO layer is made thicker which is influenced by the magnitude of the electric field in the LAO and the mismatch in dielectric constants between LAO and STO. Lowering the temperature in these systems will allow the electrons to move further away from the La:STO/LAO interface because of increased electron screening coming from higher dielectric constants in La:STO and STO at lower temperatures. By changing the La:STO layer thickness we can tune the ratio of charge carriers in the La:STO layer and STO substrate. We showed the carriers in the La:STO are localized at low temperature whereas those at the interface between STO and La:STO display high mobilities. The creation of this insulating layer allows us to move a portion of the charge carriers created at the La:STO/LAO interface to the well at the La:STO/STO interface which constitutes modulation doping.

This work shows it is possible to move electrons around in oxide materials in a similar manner as in much better understood classical semiconductor systems. It opens the door to more intricate quantum well and modulation doping structures in oxide materials where the unique properties of oxides can contribute to new oxide electronic devices.

*g.koster@utwente.nl

- ¹T. Ando, A. B. Fowler, and F. Stern, *Rev. Mod. Phys.* **54**, 437 (1982).
- ²A. Tsukazaki, A. Ohtomo, T. Kita, Y. Ohno, H. Ohno, and M. Kawasaki, *Science* **315**, 1388 (2007).
- ³Y. Kozuka, M. Kim, C. Bell, B. G. Kim, Y. Hikita, and H. Y. Hwang, *Nature (London)* **462**, 487 (2009).
- ⁴T. Higuchi, Y. Hotta, T. Susaki, A. Fujimori, and H. Y. Hwang, *Phys. Rev. B* **79**, 075415 (2009).
- ⁵H. P. R. Frederikse and W. R. Hosler, *Phys. Rev.* **161**, 822 (1967).
- ⁶A. Ohtomo and H. Y. Hwang, *Nature (London)* **427**, 423 (2004).
- ⁷A. Ohtomo and H. Y. Hwang, *Nature (London)* **441**, 120 (2006).
- ⁸M. Huijben, A. Brinkman, G. Koster, G. Rijnders, H. Hilgenkamp, and D. Blank, *Adv. Mater.* **80**, 1665 (2008).
- ⁹G. Koster, B. L. Kropman, G. J. H. M. Rijnders, D. H. A. Blank, and H. Rogalla, *Appl. Phys. Lett.* **73**, 2920 (1998).
- ¹⁰N. J. C. Ingle, R. H. Hammond, M. R. Beasley, and D. H. A. Blank, *Appl. Phys. Lett.* **75**, 4162 (1999).
- ¹¹See supplementary material at <http://link.aps.org/supplemental/10.1103/PhysRevB.81.241308> for (a) information regarding the quality of the samples including RHEED specular spot intensity oscillations during deposition and an atomic force micrograph

taken after growth, (b) sheet resistance of films with different LAO thicknesses on top of 5 ML La:STO to be compared to Fig. 2(a) where 10 ML La:STO was deposited, and (c) hysteretic effects measured in the sheet resistance during warming at specific temperatures, which could point to the origin of the charge carriers at the LAO/La:STO interface.

- ¹²L. J. van der Pauw, *Philips Tech. Rev.* **20**, 220 (1958).
- ¹³S. Thiel, G. Hammerl, A. Schmehl, C. W. Schneider, and J. Mannhart, *Science* **313**, 1942 (2006).
- ¹⁴M. Huijben, G. Rijnders, D. H. A. Blank, S. Bals, S. V. Aert, J. Verbeeck, G. V. Tendeloo, A. Brinkman, and H. Hilgenkamp, *Nature Mater.* **5**, 556 (2006).
- ¹⁵T. Okuda, K. Nakanishi, S. Miyasaka, and Y. Tokura, *Phys. Rev. B* **63**, 113104 (2001).
- ¹⁶W. Siemons, G. Koster, H. Yamamoto, W. A. Harrison, G. Lucovsky, T. H. Geballe, D. H. A. Blank, and M. R. Beasley, *Phys. Rev. Lett.* **98**, 196802 (2007).
- ¹⁷Y. Segal, J. H. Ngai, J. W. Reiner, F. J. Walker, and C. H. Ahn, *Phys. Rev. B* **80**, 241107 (2009).
- ¹⁸R. Moos and K. H. Hardtl, *J. Appl. Phys.* **80**, 393 (1996).
- ¹⁹Z. Yu, C. Ang, and L. E. Cross, *Appl. Phys. Lett.* **74**, 3044 (1999).